Evidence for abnormalities of cortical development in Adolescent-Onset Schizophrenia

Natalie L. Voets, Morgan Hough, Gwenaelle Douaud, Paul M. Matthews, Anthony James, Louise Winmill, Paula Webster, Stephen Smith

PII: S1053-8119(08)00933-6
DOI: doi: 10.1016/j.neuroimage.2008.08.013
Reference: YNIMG 5652

To appear in: *NeuroImage*

Received date: 8 April 2008
Revised date: 12 August 2008
Accepted date: 14 August 2008

Please cite this article as: Voets, Natalie L., Hough, Morgan, Douaud, Gwenaelle, Matthews, Paul M., James, Anthony, Winmill, Louise, Webster, Paula, Smith, Stephen, Evidence for abnormalities of cortical development in Adolescent-Onset Schizophrenia, *NeuroImage* (2008), doi: 10.1016/j.neuroimage.2008.08.013

TITLE PAGE

Evidence for abnormalities of cortical development in Adolescent-Onset Schizophrenia

Natalie L. Voets*[1,3], Morgan Hough*[1], Gwenaelle Douaud[1], Paul M. Matthews[1,3,4], Anthony. James[2], Louise Winmill[2], Paula Webster[2], Stephen Smith[1]

* these authors contributed equally to this work

[1]FMRIB Centre, Department of Clinical Neurology, University of Oxford

[2]Highfield Adolescent Unit, Warneford Hospital, Oxford

[3] GlaxoSmithKline Clinical Imaging Centre, Clinical Pharmacology and Discovery Medicine, Hammersmith Hospital, London

[4] Department of Clinical Neurosciences, Imperial College, London

Corresponding author: natalie@fmrib.ox.ac.uk

Corresponding address: FMRIB Centre, John Radcliffe Hospital, Headington, Oxford OX3 9DU

Tel: 020 8008 6051

Fax: +44 (0) 1865 222 717

Abstract: 210

Article Word Count: 4713

Figures: 4 (+ 3 supplementary)

Tables: 8

Keywords: schizophrenia, MRI, cortical thinning, density, surface area

ABSTRACT

Voxel-Based Morphometry (VBM) identifies differences in grey matter brain structure in patients with schizophrenia relative to healthy controls, with particularly prominent differences found in patients with the more severe, adolescent-onset form of the disease. However, as VBM is sensitive to a combination of changes in grey matter thickness, intensity and folding, specific neuropathological interpretations are not possible. Here, we attempt to more precisely define cortical changes in 25 adolescent-onset schizophrenic patients and 25 age- and sex-matched healthy volunteers using Surface-Based Morphometry (SBM) to disambiguate the relative contributions of cortical thickness and surface area differences to changes in regional grey matter (GM) density measured with VBM. Cortical changes in schizophrenia were widespread, including particularly the prefrontal cortex and superior temporal gyrus. Nine regions of apparent reduction in GM density in patients relative to healthy matched controls were found using VBM that were not found with SBM-derived cortical thickness measures. In Regions of Interest (ROIs) derived from the VBM group results, we confirmed that local surface area differences accounted for these VBM changes. Our results emphasize widespread, but focally distinct cortical pathology in adolescent-onset schizophrenia. Evidence for changes in local surface area (as opposed to simply cortical thinning) is consistent with a neurodevelopmental contribution to the underlying neuropathology of the disease.

INTRODUCTION

Neuropathological changes have been an increasing focus of research in efforts to understand the aetiology of schizophrenia. Several detailed reviews highlight the current knowledge concerning the neurobiological basis of the disease (e.g. e.g. Harrison 1999; Harrison & Weinberger 2005; Glantz et al 2006). Histopathological studies report changes in neuron size and/or number in several regions, including the hippocampus, anterior cingulate cortex and dorsolateral prefrontal cortex (see Harrison 1999). Alterations in neuronal presynaptic markers and dendritic density (arborisation) and altered GABAergic, glutamatergic and dopaminergic neurotransmission have been interpreted as evidence for impaired functional connectivity, possibly arising from abnormal neurodevelopment (Roberts 1990, Harrison 1997, 1999, Lewis & Lieberman 2000). There are associated microscopic grey and white matter structural changes, but evidence for larger-scale patterns of cortical volume loss has been less consistent. Postmortem results have suggested prefrontal and anterior cingulate cortical density changes (see Glantz et al 2006), with inconsistent reports of reduced volume in thalamic subregions, the temporal lobes and cerebellum, and increased volume of the basal ganglia (for a review see Harrison 1999, Shapiro 1993). Attempts to relate specific brain structural changes to disease symptoms or progression have been equivocal (Harrison & Wienberger 2005, Harrison 1999).

Since the advent of non-invasive imaging techniques (Magnetic Resonance Imaging (MRI) in particular), several hundred studies examining volumetric brain changes in schizophrenic populations have been reported. A review of 15 studies published in 2004 alone revealed large heterogeneity in reported structural changes as detected using voxel-based morphometric (VBM) analyses of MRI data collected in schizophrenic subjects (Honea et al., 2005). The review highlighted that, of over 50 reportedly affected regions, only 2 regions were noted consistently in more than 50% of the studies: the left medial temporal lobe and the left superior temporal gyrus. Half of the studies also found grey matter (GM) density reductions in patients relative to controls in the left inferior and medial frontal gyri, left parahippocampal gyrus and right superior temporal gyrus.

Limitations in both data acquisition (e.g. resolution) and analysis approaches (e.g. intensity-based segmentation techniques, optimal smoothing and biologically-meaningful spatial normalisation between subjects) may confound interpretation of MRI-derived atrophy estimates. VBM analyses in particular are sensitive to the degree of smoothing, differences in registration and choice of normalization template (Jones et al., 2005; Bookstein, 2001; Park et al., 2004). Surface-Based Morphology (SBM) analysis approaches have been put forward as an alternative method for probing cortical grey matter group changes, and additionally allow the contributions of grey matter thinning and regional surface area (which are confounded in VBM approaches) to be defined independently. Another source of variability in cortical volume changes in schizophrenic subjects is choice of patient population. Gender (Im et al. 2006, Walder et al., 2007), age at onset (Narr et al., 2005a; Nugent et al., 2007) and medication (Glenthoj et al. 2007; Gur et al 1998; Khorram et al 2006; Lang et al., 2004; McClure et al., 2006), for example, have all been shown to influence cortical volume (Walder et al 2006, 2007; Narr et al 2005a, Nugent et al 2007; Glenthoj et al 2007, Lang et al 2004, Gur et al 1998, McClure et al 2006, Khorram et al 2006).

In this study, we assess cortical changes in schizophrenic patients (selected for recent, adolescent-onset to minimise population heterogeneity) relative to age- and gender-matched healthy controls. Results from surface-based and voxel-based morphometry analysis approaches are compared to differentiate cortical thinning from local changes in surface area in regions where disease-associated GM changes were found. We first present results of separate SBM-derived cortical thickness and VBM-derived density analyses that contrast adolescent-onset patients with healthy volunteers. Subsequently, we describe global and regional SBM measures of surface area change, and relate these to the cortical density change results. Finally, we test the power of SBM and VBM measures to discriminate between healthy controls and patients.

MATERIALS AND METHODS

Subjects

Twenty-five adolescent-onset schizophrenics (18 males, aged 13 to 18, mean age 16.25 (stdev 1.4)) were recruited from the Oxford Regional Adolescent Unit and surrounding units. All met DSM IV (APA, 1994) criteria for schizophrenia, based on the Kiddie Schedule for Affective Disorders and Schizophrenia

(Kaufman et al, 1997). Age at onset of symptoms ranged from 11-17 years (mean: 15 ± 1.5 years). All patients were receiving atypical neuroleptics. Twenty-five age and sex-matched healthy volunteers were also recruited (17 men, age range: 13-19 years, mean age 16 (+/- 1.5)). Handedness was assessed with the Edinburgh Handedness Questionnaire (Olfield, 1971). All participants attended normal schools. Subjects with a history of substance abuse or pervasive developmental disorder, significant head injury, neurological disorder or major medical disorder were excluded. Full score IQ differed significantly between the groups ($p<0.001$). Participant demographics are presented in **Table 1**.

The study was approved by the Oxford Psychiatric Research Ethics Committee. Informed written consent was obtained from all participants or their legal custodian.

Data Acquisition

T1-weighted whole-brain structural images were acquired for all subjects on a 1.5 T Siemens Sonata MR scanner using a 3D FLASH sequence (TR 12ms, TE 5.6ms, matrix 256×256x208, 1x1x1mm resolution, 1 average).

Image Analysis

Cortical surface generations and thickness estimation

Surface-based analysis was conducted using FreeSurfer tools (http://surfer.nmr.mgh.harvard.edu/) (Dale et al., 1999; Fischl et al. 1999 a,b). . Individual subject's T1 volumes were linearly aligned to the MNI 305 average brain template, bias corrected, skull stripped, and segmented into tissue types. The segmented white matter (WM) volume was used to derive a tessellated surface representing the gray-white boundary. The surface was automatically corrected for topology defects, and expanded to model the pial-gray boundary to produce a second, linked mesh surface. The distance between the grey-white matter boundary and the pial mesh was used to estimate cortical thickness. The grey-white surface was then inflated to form a sphere and warped (on the sphere) to match curvature features across subjects (Dale et al., 1999; Fischl et al. 1999 a,b).. After alignment to the spherical-space standard curvature template, the cortex was partitioned using an automated Bayesian segmentation procedure designed to replicate the neuroanatomical

parcellation defined in (Desikan et al., 2006).. Each processing step was verified through: a) visual verification of segmentation and label outputs; (b) visual verification of alignment by (i) back-projection of average template sulcal ROIs to individual subject T1s and (ii) back-projection of a smaller ROI of significant group difference in the post-central region from the average template to individual subject T1 images; (c) searching for patient outliers in regional cortical thickness measures; and (d) spherical visualization of curvature after alignment. Poor data quality, limiting surface reconstruction, led to the exclusion of 1 patient and 3 control subjects from the SBM analysis.

Following surface extraction, a mean group template was generated for the 46 subjects. The gray-white surface from each subject was inflated to a sphere (Dale et al., 1999a) and nonlinearly aligned to a study-derived spherical template formed from the curvature-based registration of the subjects (Fischl et al., 1999a) . The contribution of potential gender and handedness differences within the complete dataset of 46 participants was assessed by creating a template for a subset of only right-handed male subjects (15 controls/15 patients), as this specific template might be expected to improve alignment by better matching curvature asymmetries within this gender subgroup.

A cross-subject general linear model (GLM), fit at each vertex, was used to test group-wise differences in surface measures between schizophrenic patients and healthy volunteers. Individual subject thickness measures were smoothed using a full width half maximum (FWHM) kernel of 10mm, and compared with results for 5mm, 15mm, 20mm, 25mm and 30mm. Group difference t-stat maps were false-discovery-rate (FDR) corrected (for multiple comparisons across vertices) at $p<0.05$ (Genovese et al., 2002). .GLM analysis was also repeated in the patient group using neuroleptic dose (chlorpromazine equivalent dose) as a regressor to examine potential drug effects on cortical thickness (see Bezchlibnyk-Butler and Jeffries (2000)).

Surface-based parcellation

Subject-specific cortical parcellations were automatically generated through nonlinear surface registration of each subject's curvature measures to a reference surface template generated from 40 healthy subjects

(Desikan et al., 2006), with subsequent Bayesian segmentation of the surface features based on the statistics extracted from the manually labelled regions, optimised for each subjects' specific curvature, to the aligned surface (for a more detailed description, see Fischl et al. 2004a). This automated parcellation was used to report results, provide a regional decomposition for surface area testing, and constrain subject discrimination to regions of significant disease effects.

Surface-based metric distortion analysis

Subject-specific spherical deformation measures were generated from each individual subject's surface warp field, reflecting – at each point on the inflated surface mesh – the extent of local area expansion/contraction required to align the individual's surface to the group average template. Metric distortion measures were smoothed with a 10mm FWHM kernel and tested for group differences both using the raw values, and after scaling (normalizing) by the ratio of the global surface area change.

Surface area analysis

Smoothness constraints in the nonlinear surface warp may render metric distortion relatively insensitive to subject-wise variations in local surface area. Regional surface area measures are complementary and derived from native images; these were obtained from the cortical parcellations described above. The average surface area of the white and pial surfaces was computed and used to approximate the midway surface area, which was then summed for each parcellation.

VBM-style analyses

A detailed description of a VBM-style analysis of the same subjects is reported in Douaud et al. (2007). Briefly, whole-brain voxel-wise differences in GM morphometry between adolescent schizophrenic patients and healthy volunteers were tested using an "optimised" FSL-based VBM approach using FSL tools (Good et al., 2002; Smith et al., 2004, www.fmrib.ox.ac.uk/fsl), compensating for possible contraction or enlargement due to the nonlinear element of data alignment. The individual modulated normalised GM density images were smoothed with an isotropic Gaussian kernel of approximately 8 mm FWHM. Differences in the distribution of GM between the patient and healthy volunteer groups were examined

using permutation-based non-parametric inference testing (Nichols et al., 2002) . Results were considered significant at $p<0.05$ (5000 permutations, initial cluster-forming thresholding at P-uncorrected=0.05), fully corrected for multiple comparisons. This analysis was repeated, including a regression analysis with medication (chlorpromazine equivalent dose) to test for effects of atypical neuroleptics on measures of structural abnormality.

Surface Scaling Factors

As differences in brain size may bias cortical thickness estimates (Luders et al. 2006), we analyzed the data with and without corrections for individual differences in brain size. The scaling of a subject's skull-stripped brain to the template was calculated from the linear transformation matrix produced by FSL's FLIRT (Jenkinson and Smith, 2002) and used to provide global scaling/normalisation for some of the surface-based results (e.g. cortical thickness). As average scaling is a 3D measure of brain size, cortical thickness was corrected with the $1/3^{rd}$ power of average scaling while area was corrected with the $2/3^{rd}$ power.

An additional measure of overall brain size is FreeSurfer's intracranial volume (ICV) estimate based on Buckner et al. (2004). Both brain size measures were tested for between-group differences. Surface models also provide overall cortical estimates such as total surface area and global mean cortical thickness, which may be better suited to scale regional SBM-derived measures. Mean cortical thickness was also used to normalise the surface-based measures and assess the differences with traditional volumetric scaling.

All statistical tests were conducted using Walsh's t-test in R (Venables & Ripley 1999).

VBM ROI rendering onto SBM-derived average surface

VBM-style approaches are sensitive to a combination of cortical thickness, surface area and shape measures. SBM, on the other hand, uses an explicit model of the neocortex, offering independent measures of thickness, surface area and folding patterns. Thus, areas of significant difference in VBM GM density may be found without a corresponding change in SBM-derived cortical thickness. To visualise differences

in anatomical location of GM group changes between the two analysis methods, the thresholded VBM-derived group difference t-statistic map was rendered onto the SBM-based average surface template by first "inverse-warping" the VBM group difference map to the native-space T1 structural image of each of the 46 individual subjects used in the SBM analysis. Subsequently, for each subject, the resulting ROI was forward-warped to spherical surface standard space through the same transformation used to bring individual subjects' grey matter into alignment with the average template.

SBM and VBM Discriminant Testing

Linear discriminant analysis (LDA) was conducted on SBM-derived thickness and metric distortion estimates and the smoothed and modulated GM images. Multivariate VBM, and both univariate and multivariate SBM discriminant testing was conducted voxel/vertex-wise using a leave-one-out cross-validation (LOOCV) approach to form a discriminant scalar or vector from N-1 subjects and testing this on the subject left out (Hastie et al., 2001).

In order to assess the spatial sparsity of the discrimination, mean cortical thickness, curvature, surface area and volume measures derived from each of the 32 cortical regions of the Desikan template (Desikan et al., 2006) were paired with the same estimate from each of the other regions following Lerch et al. (2006), and LDA was performed as a simple 2D multivariate discriminant analysis.

As a secondary surface-based discriminant analysis, we also subdivided the largest parcellation areas (IT, MT, ST, PreC, PostC, and Superior and Rostral Frontal) into 3 - or in the case of the "superior frontal" label - 4 regions of equal area along the principal axis of the parcel in order to improve the spatial sensitivity of the LDA discriminant analysis.

RESULTS

Surface-based Morphometry (SBM) results: global summary measures and scaling factors

Significant differences in volumetric brain size were found between the patient and control groups (Table 2). There were also significant differences in GM volume, WM surface area, mean cortical thickness and the ratio of gyral-sulcal WM surface.

Surface-based Morphometry results: Cortical volume changes

Group t-stat maps derived from surface-based analysis revealed significantly decreased cortical thickness in adolescent-onset schizophrenic patients relative to healthy controls in several cortical regions across the brain. These included bilateral caudal middle frontal, precuneus, superior parietal, superior temporal, lingual, postcentral and paracentral regions. Left hemisphere thinning was localised to pars opercularis, lateral orbitofrontal sulcus, cuneus, inferior parietal sulcus, and an unlabelled region in the insula. Right hemisphere cortical thinning was observed in the lateral occipital gyrus, posterior inferior temporal gyrus, rostral middle frontal, superior frontal, posterior cingulate gyrus and an unlabelled region in the parietal operculum/postcentral border (Figure 1, Table 3). No regions of increased thickness were found in patients relative to controls. The overall spatial distribution of cortical thinning was independent of smoothing kernels between 5-30mm FWHM.

We tested for independent effects of neuroleptic medication by modelling chlorpromazine equivalent dose as an explanatory variable in the SBM GLM model. No significant medication-related cortical thickness differences were found. Modelling IQ as an explanatory variable reduced the overall effect size of the results (as IQ differed significantly between the groups) but did not alter the spatial distribution of the results.

Voxel-based morphometry results

Detailed voxel-based morphometry results were reported previously (Douaud et al., 2007) and are reproduced here (Figure 2A) for comparison with SBM results (Figure 2B). No regions of increased GM density were found for patients relative to controls.

VBM-SBM comparisons: co-localisation of significant results

Comparison of SBM and VBM results identified overlapping density (decreased in patients) and cortical thickness changes (thinning in patients) (Figure 2, Table 4a) in the left hemisphere superior parietal/postcentral border, pars opercularis, superior temporal/insula border, precuneus and

precuneus/paracentral border. In the right hemisphere, regions of overlap were found in the rostral middle frontal/superior frontal gyri, superior temporal/insula border, inferior temporal sulcus/gyrus border, superior parietal cortex, medial superior frontal sulcus/gyrus border, posterior cingulate and precuneus regions.

Comparison of SBM and VBM group difference maps also revealed regions of VBM GM density change in which no corresponding evidence of cortical thinning was seen with SBM in the bilateral inferior/middle temporal gyrus, medial superior frontal gyrus (SMA), pre/postcentral gyrus (primary motor mouth area), posterior parietal operculum/transverse temporal (Heschl's) gyrus and rostral anterior cingulate/medial superior frontal cortex (Figure 2) (Table 4b).

VBM-SBM comparisons: metric distortion

As changes in local surface area might explain discrepancies between VBM and SBM measures, we first tested relative local distortion measures for potential group differences. Spherical deformation maps revealed differences in the expansion/contraction of the warp field between patients and controls (Figure 3), but did not survive multiple comparisons correction. Employing alternative smoothing levels (5-35mm smoothing FWHM) did not significantly affect the results.

The analysis was extended by testing whether the combined measure of cortical thickness and metric distortion approximated VBM density changes (see supplementary material). While the combined measures maps better approximated the VBM maps, significant differences remained (supplementary Figure S1).

VBM-SBM comparison: surface area measures

The lack of clear correspondence between the vertex-wise SBM measures and VBM-density measures suggests that metric distortion alone may not offer a sufficiently sensitive measure of underlying surface area change. We therefore used *regional surface area measures* extracted from the Desikan template parcellations in the native structural images to test for differences between adolescent-onset schizophrenics

and healthy volunteers. This revealed significant surface area differences between the groups in several regions co-localising with those showing VBM density changes but no corresponding SBM thickness change (Table 5). More refined localisation to test whether surface area changes underlie, for instance, the VBM SMA result, was limited by the lack of spatial detail provided by the large template parcellations.

VBM ROI-constrained Analysis of SBM estimates to derive local cortical area

Due to the lack of spatial specificity of parcellation-derived surface area measures, we finally sampled surface area directly within regions of interest (ROI) defined based on the VBM results. Each of the 9 VBM regions not showing group-wise SBM thickness change was unwarped back to each subject's native (T1) image. The native space ROIs were then projected onto the midthickness surface, spatially normalised via nonlinear spherical registration, and averaged (across subjects). (An example of the VBM Heschl's ROI is depicted in Supplementary Material Figure S2). Within each projected ROI, surface measures were sampled from the GM mid-surface estimates (Table 6a,b). Thickness measures were also sampled as before. T-tests conducted on surface area measures sampled from VBM ROIs revealed significant differences in schizophrenic patients relative to healthy volunteers in all 9 regions distinguished in the VBM- and SBM-based patient-control contrast.

The effect of global disease-related cortical volume decreases on local estimates

As brain sizes differed significantly between patients and controls, surface area measures sampled from VBM-derived ROIs could be confounded by global size differences. The computed mask size, reflecting the size of the ROI created on the MNI template, applied to the individual control and patient brains, might therefore differ between the two populations. However, scaled mask sizes remained significantly different between patients and controls, suggesting global size difference alone did not account for the local mask size differences in these regions.

Discriminant Analysis

The observation of structural differences between brains of patients with schizophrenia and healthy controls at the group level suggested that individual subjects could be classified based on these differences.

Multivariate discriminant analysis using the VBM smoothed modulated GM images yielded 84% accuracy in classifying subjects as healthy volunteer or adolescent schizophrenic patient (42/50 subjects correctly classified), with 88% sensitivity and 80% specificity. Surface-based discriminant analysis was performed using two approaches. Vertex-wise discrimination using cortical thickness yielded 84% accuracy (Figure 4). The second approach, using cortical thickness measures derived from paired, or subdivided Desikan parcels, offered a similar level of discrimination (82% accuracy between groups using paired parcels; up to 87% using sub-divided parcels).

DISCUSSION

We set out to determine specific measures contributing to altered cortical density in adolescent-onset schizophrenic patients relative to age- and sex-matched healthy volunteers. By estimating surface-derived thickness and surface area changes, we anticipated being able to interpret VBM-derived density changes more precisely. We hypothesized that VBM density analysis would reveal additional regions of group-wise change compared with SBM thickness measures, due to the confound of local area change in the VBM density estimate. Consistent with this, we observed both common regions of cortical change using SBM and VBM analysis methods (pre/postcentral, temporal and frontal lobe regions), and regions in which VBM group density changes were found that were not accompanied by corresponding SBM thickness change. Smoothing levels, metric distortion analysis, or analysis using a volume change estimate to approximate VBM results were unable to fully account for the differences in results between the methods. However, local surface area was significantly different in all regions showing VBM-density but not SBM thickness change in adolescent-onset schizophrenia. These results (i) highlight that surface-based methods can provide sensitive, relatively interpretable, indices of disease-related structural changes, and (ii) demonstrate that both relative cortical thinning and local surface area changes characterise the neuropathology of adolescent-onset schizophrenia. The latter are consistent with underlying neurodevelopmental differences between schizophrenia and healthy controls.

Grey matter changes found with both VBM and SBM are consistent with cortical thinning

Grey matter cortical changes independent of the analysis method used involved the left hemisphere prefrontal cortex and precuneus, and right hemisphere precuneus and superior/middle temporal regions. This suggests cortical thinning as the primary measure underlying cortical changes in these regions, and is consistent with recent reports of prefrontal lobe cortical thinning (Kuperberg et al 2003, Narr et al 2005a, b), potentially also involving temporal and parietal regions (see Greenstein et al., 2006). Our findings of cortical thinning in left hemisphere prefrontal, and right hemisphere superior/middle temporal regions are consistent with reports of progressive frontal and temporal lobe volume loss (Farrow et al., 2005; Gur et al. 1998; Mathalon et al., 2001, see Nakamura et al. 2007 for review), and progressive changes exceeding those seen in non-psychotic siblings (Honea et al., 2007). As SBM measures of cortical thinning, consistent with VBM density change in these regions, may reflect cortical lamination changes (Makris et al., 2006), our results are consistent with thalamo-cortical neurodevelopmental abnormalities preferentially affecting medial dorsal thalamus connections with frontal and temporal cortical regions (Mitelman et al., 2005c).

It is likely that these cortical changes have behavioural correlates. Functional-anatomical correlates of structural measures with symptoms of schizophrenia have been found in superior temporal (Wright et al., 1995, Mitelman et al., 2005a) and frontal lobe (e.g. Mitelman et al., 2005b) regions. Previously, we found changes in white matter integrity along the arcuate fasciculus consistent with changes in both VBM density (Douaud et al., 2007) and SBM thickness in left inferior frontal gyrus, a region potentially implicated in auditory hallucinations (Garcia-Marti et al., 2007, but see Gaser et al., 2004).

Grey matter changes detected with VBM but not SBM suggest locally reduced cortical surface area in patients

Measures of grey matter density in VBM are a mixture of thickness, surface area and folding differences. SBM, in contrast, fits surfaces to the gray/white and pial boundaries, and for each hemisphere separately. Our second observation of bilateral GM density changes in VBM, not detected with SBM, suggests regional differences in local cortical surface area in adolescent-onset schizophrenic patients relative to

controls. We used four approaches to test this theory. The Jacobian of the warp field demonstrated regional change in some of the VBM density change regions, but did not survive FDR thresholding. More directly approximating the VBM-derived density measure using an additional measure of volume change - obtained by dividing cortical thickness by change in metric distortion at every vertex - improved sensitivity relative to analysis using each measure separately, but did not fully explain the difference between VBM and SBM results. A surface area measure derived from the anatomic labels on the surface template identified significant surface area differences in several of the labels. However, the large extent of each parcellation region precluded more precise localisation of the significant surface area results. Repeating this analysis using surface area measures derived directly from each subject's native space within VBM-defined ROIs identified highly significant local surface area changes in each of the ROIs, even when these were corrected for group differences in brain size. Thus, VBM density changes in schizophrenia, not supported by cortical thinning, were attributable to altered surface area in these regions. We hypothesized that these local area changes were not seen in the FreeSurfer-derived localised measure of area change (warp field of the Jacobian) because of constraints on scale of spatial integration, affected by factors such as spatial smoothing, effective smoothness of the surface registration, and accuracy of the surface registration.

These findings support the hypothesis that abnormal cortical development contributes to the aetiology of schizophrenia. They further suggest regionally variable development of local cytoarchitectonical fields, a concept consistent with previous work (Vogeley et al 2000, Harris et al 2004a, b, Kulynuch et al 1997, Sallett et al 2003; see Wisco et al, 2007). Gyrification changes, a potential consequence of local cytoarchitectonical field abnormalities, have recently been reported in the left hemisphere pars triangularis (Wisco et al., 2007). Harris et al (2007) found right a prefrontal cortex gyrification index was highly predictive of schizophrenia risk.

Local disease-specific cortical changes can discriminate adolescent-onset schizophrenic patients from healthy volunteers

This latter study, our recent work (Douaud et al., (2007)), and that of others, suggests that cortical patterns may provide phenotypic markers specific for schizophrenia. Bilateral Heschl's gyrus/planum temporale changes may provide a consistent index. Changes in these regions have been reported at first presentation of schizophrenia, while left hemisphere Heschl's gyrus shows progressive change with disease duration (Kasai et al 2007). Moreover, structural changes correlate with both severity of auditory hallucinations (Gaser et al 2004) and progressive changes in mismatch negativity (Salisbury et al. 2007). The relevance of altered shape compared with cortical thickness in this region to schizophrenia risk and symptoms presentation warrants further investigation.

We investigated this hypothesis here more generally. Our discriminant analysis results suggested that patients and healthy controls could be discriminated well based on either VBM (84%) or SBM (84%) measures. For the SBM parcel-based approach, eleven regions (paired parcels) showed high discriminant ability between patients and controls. In various combinations, these were the banks of the superior temporal sulcus (BSTS), lingual gyrus, medial orbital frontal, pars opercularis, posterior cingulate gyrus and precuneus. The highest discrimination was obtained with the combination of left BSTS with right paracentral region, left cuneus with right BSTS, and left medial orbitofrontal with right posterior cingulate labels. This is consistent with a central role for superior medial temporal thickness pathology in schizophrenia (Lawrie 2007).

Methodological considerations

The sample size of our study is relatively small compared with adult-onset schizophrenia studies, limiting the interpretation of our findings in the wider context of the neuropathology of schizophrenia. However, the prevalence of schizophrenia in our onset-group is lower than in adulthood. Our sample may therefore be relatively characteristic, and is comparable to other studies in this population. Future studies in larger samples will be needed to determine possible relationships between disease symptoms and local structural changes. Cortical folding differences may exist between male and female subjects, particularly in the left frontal lobe (Im et al. 2006, Luders et al. 2007). Although our subject groups were matched for sex, subtle gender-specific spatial registration differences or sex-by-disease trait interactions remain possible. In our

previous study, we repeated density analysis on the same analysis on a 15 control/15 patient subset of right-handed males (Douaud et al., 2007). Repeating the SBM thickness analysis using the same subset of male subjects revealed the same distribution of cortical thinning as seen in the mixed-sex larger group, albeit with reduced significance due to the smaller number of subjects. Including gender as an additional regressor in the GLM analysis did not significantly alter the spatial distribution of thinning results. Neuroleptics have also previously been reported to impact on cortical density measures. Neuroleptic dose, however, was not correlated significantly with either local cortical density or local thickness measures in our analyses.

Reduced brain size in schizophrenic patients relative to controls may confound local estimates of volume change. We attempted to address this in our study through correction of locally-sampled measures by scaling mask sizes using the overall measure of brain size (scaling factor) derived from linearly registering skull-stripped volumes. This measure is more appropriate than skull-derived measures in cases where CSF differences exist (such as in schizophrenia) However, the scaling factor lacks tissue differentiation, and therefore may not correct for developmental biases in tissue volume (grey versus white matter).

Conclusions

In this study, we identified significant, regionally variable cortical pathology in adolescent-onset schizophrenia, consistent with anatomically specific neurodevelopmental impairments. Anatomically distinct changes in local cortical surface area and cortical thinning offer evidence for potentially regionally distinct neurodevelopmental consequences – thinning (perhaps related to loss of neuropil or altered pruning) and altered regional cytoarchitectonic area. We further demonstrated the potential for these changes to discriminate patients from healthy controls. Evidence from a range of reports suggests that symptom presentation may be related to heterogeneity in the pattern of brain changes. In future work it will be important to define the longitudinal trajectory of these abnormalities and their relationship to disease symptomatology.

ACKNOWLEDGEMENTS

We would like to thank the UK Medical Research Council (MRC) for funding this research, the patients and volunteers who took part in this study, Bruce Fischl and, Paul Harrison for helpful suggestions on analysis methods and this manuscript. NV and PMM are fulltime employees of GlaxoSmithKline.

REFERENCES

Bezchlibnyk-Butler KZ and Jeffries JJ, editors (2000): Clinical Handbook of Psychotropic Drugs, 10th ed. Seattle: Hogrefe & Huber Publishers, pp.84-88

Bookstein FL. (2001). "Voxel-based morphometry" should not be used with imperfectly registered images. Neuroimage, 14(6):1454-62.

Buckner et al. (2004) A unified approach for morphometric and functional data analysis in young, old, and demented adults using automated atlas-based head size normalization: reliability and validation against manual measurement of total intracranial volume. NeuroImage 23:724-738.

Dale, AM, Fischl, B, Sereno, MI. (1999). Cortical Surface-Based Analysis I: Segmentation and Surface Reconstruction. NeuroImage 9(2):179-194

Desikan RS, Segonne F, Fischl B, Quinn BT, Dickerson BC, Blacker D, Buckner RL, Dale AM, Maguire RP, Hyman BT, Albert MS, Killiany RJ. An automated labeling system for subdividing the human cerebral cortex on MRI scans into gyral based regions of interest. Neuroimage. 2006 Jul 1;31(3):968-80.

Douaud G, Smith S, Jenkinson M, Behrens T, Johansen-Berg H, Vickers J, James S, Voets N, Watkins K, Matthews PM, James A. (2007). Anatomically related grey and white matter abnormalities in adolescent-onset schizophrenia. Brain. 130(Pt 9):2375-86.

Farrow TF, Whitford TJ, Williams LM, Gomes L, Harris AW. (2005). Diagnosis-related regional gray matter loss over two years in first episode schizophrenia and bipolar disorder. Biol Psychiatry, 58(9):713-23.

Fischl, B, Sereno, MI, Dale, AM. (1999a). Cortical Surface-Based Analysis II: Inflation, Flattening, and a Surface-Based Coordinate System. NeuroImage, 9(2):195-207.

Fischl B, Sereno MI, Tootell RB, Dale AM. High-resolution intersubject averaging and a coordinate system for the cortical surface. Hum Brain Mapp. 1999b;8(4):272-84.

Fischl, B, A. van der Kouwe, Destrieux C, Halgren E, Segonne F, Salat D, Busa E, Seidman L, Goldstein J, Kennedy D, Caviness V, Makris N, Rosen B, and Dale AM. (2004a). Automatically Parcellating the Human Cerebral Cortex. Cerebral Cortex, 14:11-22.

Garcia-Marti G, Aguilar EJ, Lull JJ, Marti-Bonmati L, Escarti MJ, Manjon JV, Moratal D, Robles M, Sanjuan J. (2007). Schizophrenia with auditory hallucinations: A voxel-based morphometry study. Prog Neuropsychopharmacol Biol Psychiatry.

Gaser C, Nenadic I, Volz HP, Buchel C, Sauer H. (2004). Neuroanatomy of "hearing voices": a frontotemporal brain structural abnormality associated with auditory hallucinations in schizophrenia. Cereb Cortex, 14(1):91-6.

Genovese CR, Lazar NA, Nichols T. (2002) Thresholding of statistical maps in functional neuroimaging using the false discovery rate. Neuroimage, 15(4):870-8.

Giedd JN, Blumenthal J, Jeffries NO, Castellanos FX, Liu H, Zijdenbos A, Paus T, Evans AC, Rapoport LJ (1999). Brain development during childhood and adolescence: a longitudinal MRI study. Nature Neuroscience 2(10): 861-863.

Glantz LA, Gilmore JH, Lieberman JA, Jarskog LF. (2006). Apoptotic mechanisms and the synaptic pathology of schizophrenia. Schizophr Res. 81(1):47-63.

524 Glenthoj A, Glenthoj BY, Mackeprang T, Pagsberg AK, Hemmingsen RP, Jernigan TL, Baare WF (2007).
525 Basal ganglia volumes in drug-naïve first-episode schizophrenia patients before and after short-term
526 treatment with either a typical or an atypical antipsychotic drug. Psychiatry Res 154(3): 199-208.
527
528 Good CD, Scahill RI, Fox NC, Ashburner J, Friston KJ, Chan D, Crum WR, Rossor MN, Frackowiak RS
529 (2002). Automatic differentiation of anatomical patterns in the human brain: validation with studies of
530 degenerative dementias. Neuroimage 17(1): 29-46.
531
532 Greenstein D, Lerch J, Shaw P, Clasen L, Giedd J, Gochman P, Rapoport J, Gogtay N (2006). Childhood
533 onset schizophrenia: cortical brain abnormalities as young adults. J Child Psychol and Psychiatry 47(10):
534 1003-1012.
535
536 Gur RE, Maany V, Mozley PD, Swanson C, Bilker W, Gur RC (1998). Subcortical MRI volumes in
537 neuroleptic-naïve and treated patients with schizophrenia. Am J Psychiatry 155(12): 1711-7.
538
539 Hamilton LS, Narr KL, Luders E, Szeszko PR, Thompson PM, Bilder RM, Toga AW. (2007).
540 Asymmetries of cortical thickness: effects of handedness, sex, and schizophrenia. Neuroreport. 2007 Sep
541 17;18(14):1427-31.
542
543 Harris JM, Moorhead TW, Miller P, McIntosh AM, Bonnici HM, Owens DG, Johnstone EC, Lawrie SM.
544 (2007). Increased prefrontal gyrification in a large high-risk cohort characterizes those who develop
545 schizophrenia and reflects abnormal prefrontal development. Biol Psychiatry, 62(7):722-9.
546
547 Harris JM, Whalley H, Yates S, Miller P, Johnstone EC, Lawrie SM (2004). Abnormal cortical folding in
548 high-risk individuals: a predictor of the development of schizophrenia? Biol Psychiatry 56(3): 182-9.
549
550 Harrison P.J. (1999). The neuropathology of schizophrenia. Brain 122(Pt4): 593-624
551

552 Harrison P.J. (1997). Schizophrenia: a disorder of neurodevelopment? Curr Opin Neurobiol. 7(2):285-9.

553

554 Harrison P.J. & Weinberger D.R. (2005). Schizophrenia genes, gene expression and neuropathology: on the
555 matter of their convergence. Mol Psychiatry 10(1): 40-68

556

557 Hastie T, Tibshirani R, Friedman J. (2001). The Elements of Statistical Learning: Data Mining, Inference,
558 and Prediction, Springer

559

560 Honea RA, Meyer-Lindenberg A, Hobbs KB, Pezawas L, Mattay VS, Egan MF, Verchinski B, Passingham
561 RE, Weinberger DR, Callicott JH. (2007). Is Gray Matter Volume an Intermediate Phenotype for
562 Schizophrenia? A Voxel-Based Morphometry Study of Patients with Schizophrenia and Their Healthy
563 Siblings. Biol Psychiatry.

564

565 Honea R, Crow TJ, Passingam D, Mackay CE (2005). Regional deficits in brain volume in schizophrenia :
566 a meta-analysis of voxel-based morphometry studies. Am J Psych 162 (12): 2233-2245.

567

568 Im K, Lee JM, Lee J, Shin YW, Kim IY, Kwon JS, Kim SI. (2006). Gender difference analysis of cortical
569 thickness in healthy young adults with surface-based methods. Neuroimage. 31(1):31-8.

570

571 Jenkinson M, Smith S. (2001). A global optimisation method for robust affine registration of brain images.
572 Med Image Anal. 5(2):143-56.

573

574 Jones DK, Symms MR, Cercignani M, Howard RJ. (2005). The effect of filter size on VBM analyses of
575 DT-MRI data. Neuroimage. 26(2):546-54.

576

577 Kasai K, McCarley RW, Salisbury DF, Onitsuka T, Demeo S, Yurgelun-Todd D, Kikinis R, Jolesz FA,
578 Shenton ME. (2004). Cavum septi pellucidi in first-episode schizophrenia and first-episode affective
579 psychosis: an MRI study. Schizophr Res., 71(1):65-76.

Kaufman J, Birmaher B, Brent D, Rao U, Flynn C, Moreci P, Williamson D, Ryan N. (1997). Schedule for Affective Disorders and Schizophrenia for School-Age Children-Present and Lifetime Version (K-SADS-PL): initial reliability and validity data. J Am Acad Child Adolesc Psychiatry. 36(7):980-8.

Khorram B, Lang DJ, Kopala LC, Vandorpe RA, Rui Q, Goghari VM, Smith GN, Honer WG (2006). Reduced thalamic volume in patients with chronic schizophrenia after switching from typical antipsychotic medications to olanzapine. Am J Psychiatry 163(11): 2005-7

Kulynych JJ, Luevano LF, Jones DW, Weinberger DR. (1997). Cortical abnormality in schizophrenia: an in vivo application of the gyrification index. Biol Psychiatry, 41(10):995-9.

Kuperberg GR, Broome MR, McGuire PK, David AS, Eddy M, Ozawa F, Goff D, West WC, Williams SC, van der Kouwe AJ, Salat DH, Dale AM, Fischl B. (2003). Regionally localized thinning of the cerebral cortex in schizophrenia. Arch Gen Psychiatry, 60(9):878-88.

Lang DJ, Kopala LC, Vandorpe RA, Rui Q, Smith GN, Goghari VM, Lapointe JS, Honer WG (2004). Reduced basal ganglia volumes after switching to olanzapine in chronically treated patients with schizophrenia. Am J Psychiatry 161(10): 1829-36.

Lawrie S (2007). Distinguishing vulnerability, prediction, and progression in the preschizophrenic brain. Arch Gen Psychiatry 64: 250-251.

Lerch JP, Pruessner J, Zijdenbos AP, Collins DL, Teipel SJ, Hampel H, Evans AC. Automated cortical thickness measurements from MRI can accurately separate Alzheimer's patients from normal elderly controls. Neurobiol Aging. 2006.

Lewis DA, Lieberman JA. Catching up on schizophrenia: natural history and neurobiology. Neuron. 28(2):325-34.

Luders E, Narr KL, Thompson PM, Rex DE, Woods RP, Deluca H, Jancke L, Toga AW. (2006). Gender effects on cortical thickness and the influence of scaling. Hum Brain Mapp., 27(4):314-24.

Luders E, Narr KL, Bilder RM, Szeszko PR, Gurbani MN, Hamilton L, Toga AW, Gaser C (2007). Mapping the relationship between Cortical Convolution and Intelligence: Effects of Gender. Cereb Cortex (in press)

Makris N, Kaiser J, Haselgrove C, Seidman LJ, Biederman J, Boriel D, Valera EM, Papadimitriou GM, Fischl B, Caviness VS Jr, Kennedy DN (2006). Human cerebral cortex: a system for the integration of volume- and surface-based representations. Neuroimage 33(1):139-53

Mathalon DH, Sullivan EV, Rawles JM, Pfefferbaum A. (1993). Correction for head size in brain-imaging measurements. Psychiatry Res., 50(2):121-39.

Mathalon DH, Sullivan EV, Lim KO, Pfefferbaum A. (2001). Progressive brain volume changes and the clinical course of schizophrenia in men: a longitudinal magnetic resonance imaging study. Arch Gen Psychiatry, 58(2):148-57.

McClure RK, Phillips R, Jazayerli R, Barnett A, Coppola R, Weinberger DR (2006). Regional change in brain morphometry in schizophrenia associated with antipsychotic treatment. Psychiatry Res 148(2-3): 121-32.

Mitelman SA, Brickman AM, Shihabuddin L, Newmark R, Chu KW, Buchsbaum MS (2005c). Correlations between MRI-assessed volumes of the thalamus and cortical Brodmann's areas in schizophrenia. Schizophrenia Research 75: 265-281.

635 Mitelman SA, Shihabuddin L, Brickman AM, Buchsbaum MS (2005a). Cortical intercorrelations of
636 temporal area volumes in schizophrenia. Schizophr Res 76(2-3): 207-29.
637
638 Mitelman SA, Buchsbaum MS, Brickman AM, Shihabuddin L (2005b). Cortical intercorrelations of
639 frontal area volumes in schizophrenia. Neuroimage 27(4): 753-70
640
641 Nakamura M, Salisbury DF, Hirayasu Y, Bouix S, Pohl KM, Yoshida T, Koo MS, Shenton ME, McCarley
642 RW. (2007). Neocortical gray matter volume in first-episode schizophrenia and first-episode affective
643 psychosis: a cross-sectional and longitudinal MRI study. Biol Psychiatry, 62(7):773-83.
644
645 Narr KL, Bilder RM, Luders E, Thompson PM, Woods RP, Robinson D, Szeszko PR, Dimtcheva T,
646 Gurbani M, Toga AW. (2007). Asymmetries of cortical shape: Effects of handedness, sex and
647 schizophrenia. Neuroimage. 34(3):939-48.
648
649 Narr KL, Bilder RM, Toga AW, Woods RP, Rex DE, Szeszko PR, Robertson D, Sevy S, Gunduz-Bruce H,
650 Wang Y-P, DeLuca H, Thompson PM (2005a). Mapping cortical thickness and gray matter concentration
651 in first episode schizophrenia. Cerebral Cortex 15:708-719.
652
653 Narr KL, Toga AW, Szeszko P, Thompson PM, Woods RP, Robinson D, Sevy S, Wang Y, Schrock K,
654 Bilder RM. (2005b). Cortical thinning in cingulate and occipital cortices in first episode schizophrenia. Biol
655 Psychiatry, 1;58(1):32-40.
656
657 Nichols TE, Holmes AP.(2002). Nonparametric permutation tests for functional neuroimaging: a primer
658 with examples. Hum Brain Mapp. 15(1):1-25.
659
660 Nugent TF, Herman DH, Ordonez A, Greenstein D, Hayashi KM, Lenane M, Clasen L, Jung D, Toga AW,
661 Giedd JN, Rapoport JL, Thompson PM, Gogtay N (2007) . Dynamic mapping of hippocampal development
662 in childhood onset schizophrenia. Schizophrenia Research 90(1-3): 62-70.

Oldfield RC. (1971). The assessment and analysis of handedness: the Edinburgh inventory. Neuropsychologia. 9(1):97-113.

Park HJ, Levitt J, Shenton ME, Salisbury DF, Kubicki M, Kikinis R, Jolesz FA, McCarley RW (2004). An MRI study of spatial probability brain map differences between first-episode schizophrenia and normal controls. Neuroimage 22(3):1231-46.

Rapoport J, Giedd JN, Blumenthal J, Hamburger S, Jeffries N, Fernandez T., Nicolson R, Bedwell J, Lenane M, Zijdenbos A, Paus T, Evans A (2007). Progressive cortical change during adolescence in childhood-onset schizophrenia. Arch Gen Psychiatry 56 : 649-654

Roberts GW. (1990). Schizophrenia: the cellular biology of a functional psychosis. Trends Neurosci. 13(6):207-11.

Rueckert D, Sonoda LI, Hayes C, Hill DL, Leach MO, Hawkes DJ. (1999) Nonrigid registration using free-form deformations: application to breast MR images. IEEE Trans Med Imaging. 18(8):712-21.

Salisbury DF, Kuroki N, Kasai K, Shenton ME, McCarley RW. (2007). Progressive and interrelated functional and structural evidence of post-onset brain reduction in schizophrenia. Arch Gen Psychiatry, 64(5):521-9.

Sallet PC, Elkis H, Alves TM, Oliveira JR, Sassi E, Campi de Castro C, Busatto GF, Gattaz WF. (2003). Reduced cortical folding in schizophrenia: an MRI morphometric study. Am J Psychiatry, 160(9):1606-13.

Segonne F, Dale AM, Busa E, Glessner M, Salat D, Hahn HK, Fischl B. (2004). A hybrid approach to the skull stripping problem in MRI. Neuroimage. 22(3):1060-75.

Shapiro RM. (1993). Regional neuropathology in schizophrenia: where are we? Where are we going? Schizophr Res. 10(3):187-239.

Smith SM. (2002). Fast robust automated brain extraction. Hum Brain Mapp., 17(3):143-55.

Smith SM, Jenkinson M, Woolrich MW, Beckmann CF, Behrens TE, Johansen-Berg H, Bannister PR, De Luca M, Drobnjak I, Flitney DE, Niazy RK, Saunders J, Vickers J, Zhang Y, De Stefano N, Brady JM, Matthews PM. (2004). Advances in functional and structural MR image analysis and implementation as FSL. Neuroimage. 23 Suppl 1:S208-19.

Venables W.N. and Ripley B.D. (19999). Modern Applied Statistics with S-PLUS. Third Edition. Springer

Vogeley K, Schneider-Axmann T, Pfeiffer U, Tepest R, Bayer TA, Bogerts B, Honer WG, Falkai P. (2000). Disturbed gyrification of the prefrontal region in male schizophrenic patients: A morphometric postmortem study. Am J Psychiatry, 157(1):34-9.

Walder DJ, Seidman LJ, Makris N, Tsuang MT, Kennedy DN, Goldstein JM (2007). Neuroanatomic substrates of sex differences in language dysfunction in schizophrenia: a pilot study. Schizophrenia Research 90(1-3): 295-301

Walder DJ, Seidman LJ, Cullen N, Su J, Tsuang MT, Goldstein (2006). Sex Differences in language dysfunction in schizophrenia. Am J Psychiatry 163(3): 470-7.

Whitford TJ, Grieve SM, Farrow TF, Gomes L, Brennan J, Harris AW, Gordon E, Williams LM. (2006). Progressive grey matter atrophy over the first 2-3 years of illness in first-episode schizophrenia: a tensor-based morphometry study. Neuroimage, 32(2):511-9.

718 Wisco JJ, Kuperberg G, Manoach D, Quinn BT, Busa E, Fischl B, Heckers S, Sorensen AG (2007).
719 Abnormal cortical folding patterns within Broca's area in schizophrenia: Evidence from structural MRI.
720 Schizophr Res. 94 (1-3): 317-37
721
722 Wright IC, McGuire PK, Poline JB, Travere JM., Murray RM., Frith CD., Frackowiak RS., Friston KJ
723 (1995). A voxel-based method for the statistical analysis of gray and white matter density applied to
724 schizophrenia. Neuroimage 2(4): 244-52.
725
726
727
728
729
730
731

732 **TABLE/FIGURE LEGENDS**

733

734 **Figure 1:** ***SBM-based cortical thickness change in adolescent-onset schizophrenia relative to matched***
735 ***healthy controls.***

736 *Figure 1 Legend: group-wise GLM analysis of cortical thickness (using globally-normalised thickness*
737 *values) in adolescent-onset schizophrenia compared with age- and gender-matched healthy volunteers*
738 *demonstrated significant grey matter thinning in patients relative to controls in many regions of cortex*
739 *(Table 3) (FDR-corrected to $p<0.05$).*

740

741 **Figure 2:** ***VBM GM density group difference map rendered onto SBM average surface***

742 *Figure 2 Legend: A. Projection of the VBM-based cortical density group difference result onto the SBM-*
743 *derived group average surface. B. SBM thickness group difference map (FDR-corrected, $p<0.05$). White*
744 *circles denote regions of density change using VBM not demonstrating reduced thickness with SBM. Green*
745 *boxes identify regions of cortical change consistent between VBM (density reduction in patients) and SBM*
746 *measures (thinning in patients).*

747

748 **Figure 3:** ***Group difference spherical deformation (metric distortion) map***

749 *Figure 3 Legend: Blue: increased metric distortion (increased Jacobian values) in adolescent-onset*
750 *schizophrenic patients relative to healthy volunteers. Red: larger Jacobian values in healthy volunteers*
751 *relative to patients ($p<0.05$ uncorrected). White circles denote regions where VBM density changes were*
752 *observed but no SBM thinning in patients relative to controls.*

753

754 ***Figure 4: SBM discriminative accuracy using scaled thickness***

755 *Figure 4 Legend: Linear Discriminant Analysis using leave-one-out cross-validation on vertex-wise*
756 *thickness measures (across subjects) projected onto the average surface template. Red-yellow regions*
757 *represent areas able to discriminate adolescent-onset schizophrenic patients from healthy controls with*
758 *>70% accuracy (maximum 84%).*

759

APPENDICES

SUPPLEMENTARY MATERIAL

Figure S1: SBM group analysis using volume change to better approximate VBM density

Figure S1 Legend: SBM analysis using a volume change measure (thickness divided by metric distortion) as a closer approximation to grey matter density estimates used by VBM. Group-wise SBM volume change results surprisingly did not match VBM results, suggesting thickness and metric distortion measures are not the primary components of VBM density estimates.

Figure S2: Probability map of the average mask of the posterior operculum cluster projected to the study-derived average template.

Figure S2 legend: This region spanned multiple labels of the Desikan template. The VBM left hemisphere Heschl's ROI, when projected to the surface average, consisted of three regions distinct in surface space, but clustered together in volume space. Projection of VBM ROIs to the average SBM group surface template demonstrated differences in modelling of each method's raw measures might contribute to discrepancy in findings in some of these regions.

Figure S3: SBM group cortical thickness, scaled for global mean cortical thickness

Figure S3 Legend: Vertex-wise cortical thickness results (FDR-corrected $p<0.05$) using global mean cortical thickness as a regressor of no interest. Red-yellow regions confirm cortical thinning in schizophrenic patients relative to controls. Regions of apparent thickening in patients relative to controls (blue) emerged when using this alternate scaling approach

781 Tables

782 **Table 1:** ***Patient and healthy volunteer demographics***

	Patients	**Healthy Controls**
Gender (Male/Female)	18/7	17/8
Age (mean, standard deviation)	16, +/- 1.4	16 +/- 1.5
IQ (mean, standard deviation)	87 +/- 14	108 +/- 15
Handedness (Right/Left)	20/5	21/4
Age at onset of symptoms	Range: 11-17 Mean: 15 +/- 1.6	NA
Disease Duration	Mean 1.4 +/- 0.7	NA
Medication	6/25 clozapine, 3/25 quetiapine, 3/25 risperidone, 16/25 olanzapine	NA
Mean duration of treatment (years)	1.1 +/- 0.7	NA
Chlorpro-mazine equivalents*	340 +/- 180	NA

783

784 Footnote: Details regarding chlorpromazine equivalents can be found in [77] Bezchlibnyk-Butler and

785 Jeffries (2000).

786 **Table 2:** ***Summary SBM-derived measures of brain differences between patients and controls***

Measure	Control	Patient	Significance (p)
3D volumetric Scaling factor from native to standard space	1.06 (+/- 0.03)	1.08 (+/- 0.03)	0.03
IntraCranial Volume (mm^3)	2110000 (+/- 297000)	1804000 (+/- 341000)	<0.01
Left area scaling factor (k)	1.09 (+/- 0.11)	1.15 (+/- 0.11)	0.07
Left White Matter Volume (mm^3)	282739 (+/- 40800)	267668 (+/- 31500)	0.18
Left Grey Matter Volume	309231 (+/- 31800)	282550 (+/- 36000)	0.01
Left White Matter Surface area (mm^2)	109021 (+/- 10700)	103581 (+/- 9600)	0.08
Left Mean Cortical Thickness (mm)	2.49 (+/- 0.07)	2.40 (+/- 0.15)	0.01
Left Gyral/Sulcal ratio	0.52 (+/- 0.01)	0.51 (+/- 0.01)	0.03
Right area scaling factor (k)	1.09 (+/- 0.11)	1.15 (+/- 0.11)	0.08
Right White Matter Volume (mm^3)	283765 (+/- 37000)	268755 (+/- 32100)	0.15
Right Grey Matter Volume	309550 (+/- 30050)	282888 (+/- 36000)	0.01
Right White Matter Surface area (mm^2)	109184 (+/- 10300)	103849 (+/- 9800)	0.08
Right Mean Cortical Thickness (mm)	2.50 (+/- 0.08)	2.40 (+/- 0.14)	0.01
Right Gyral/Sulcal ratio	0.52 (+/- 0.01)	0.51 (+/- 0.01)	0.02

787

788 Footnote: metric distortion = k* area of a triangle on a registered sphere /area of triangle on gray/white

789 interface surface.

790

791 **Table 3:** ***Surface-based differences in group thickness***

Left Hemisphere Label	**t-stat**	**MNI 305 coordinates (x, y, z)**	**Right Hemisphere Label**	**t-stat**	**MNI 305 coordinates (x, y, z)**
Lateral wall			**Lateral wall**		
Bank of Superior Temporal Sulcus	4.8	-50.9, -44.2, 4.98	Lateral Occipital	5.4	47.9, -71.7, 4.7
Caudal Middle Frontal	3.7	-25.4, -0.03, 43.9	Rostral Middle Frontal	4.2	28.9, 49.9, -1.84
Inferior/Superior Parietal border	4.1	-29.1, -60.1, 41.3	Inferior Temporal	4.4	46.4, -57.1, 0.2
Pars Opercularis	4.7	-38.9, 18.1, 19.9	Caudal Middle Frontal	3.2	37.8, 1.8, 36.5
Inferior Parietal	4.1	-31.7, -75.1, 28.3	Superior Temporal	4.0 3.6	38.4, -13.8, -4.5 58.3, -33.1, 19.7
Postcentral/supramarginal	3.9	-39.4, -27, 38.4	Superior Parietal	3.6	20, -64.9, 41.7
Lateral orbitofrontal	3.2	-31.2, 29.5, -1.7	Postcentral/Superior Parietal	3.9	25.4, -37.5, 51.8
			Postcentral	3.0	64.1, -7.4, 17.5
			Supramarginal	4.2	41.3, -35.9, 39.9
Medial wall			**Medial wall**		
Precuneus	6.2	-4.9, -50.8, 46.3	Precuneus	6.0 4.7 6.2	5.7, -63.9, 32.2 19.7, -62.9, 32.2 11.3, -47.3, 41.3
Lingual	4.5	-13.5, -49.8, -2.7	Lingual	5.3	5.2, -62.9, 7.3
Paracentral	3.4	-10.9, -30.2, 47.3	Paracentral	4.0	13.3, -32.6, 48.8
Cuneus	3.2	-4.9, -81.3, 37.1	Superior Frontal	3.9	10.9, 26.7, 29.8
			Posterior cingulate	3.9	4.9, -0.3, 36.8

792 *Table 3 Legend: LH = Left Hemisphere, RH = Right Hemisphere, MNI = Montreal Neurological Institute*

793 *Footnote: Label terms are those of the Desikan template, based on gyral boundaries commonly employed*

794 *in manual segmentations. For further information on labels,see [28].*

Table 4a*: Anatomical location of regions showing corresponding VBM-based grey matter density reductions and SBM-based cortical thinning in patients relative to controls*

Left Hemisphere Label	MNI coordinates (x, y, z)	Right Hemisphere Label	MNI coordinates (x, y, z)
Superior Parietal/Post central	-30.8, -35.9, 40.8	Rostral Middle Frontal/Superior Frontal	25.1, 42.9, 19.2
Pars Opercularis	-52.4, 13.3, 15.6	Superior Temporal/Insula	39.8, -10.9, -7.1
Superior temporal/Insula	-39.4, -14.3, -6.9	Superior Parietal	26.8, -67.5, 32.2
Precuneus	-16.4, -70, 38.1	Inferior Temporal	49.3, -51.9, -7.3
Precuneus/Paracentral	-10.7, -51.4, 38.7	Posterior Cingulate	6.2, -2.8, 37.9
		Precuneus	21.4, -66.4, 32

Footnote: MNI coordinates are presented based on the Montreal Neurological Institute MNI 305 template.

Table 4b: *Anatomical location of regions showing VBM-based grey matter density reductions but no corresponding SBM-based cortical thinning in patients relative to controls*

Left Hemisphere Label	MNI coordinates (x, y, z)	Right Hemisphere Label	MNI coordinates (x, y, z)
Inferior Temporal	-61.9, -20.9, -10.3	Middle Temporal	57.9, -7.5, -14.4
Superior Frontal	-6.9, 17.7, 45.1	Superior Frontal	5.9, 7.6, 53.9
Parietal operculum	-47.2, -17.5, 8.5	Parietal operculum	48.0, -19.9, 7.46
Pre/postcentral	-49.9, -10.6, 25.9	Pre/postcentral	55.8, -18.4, 25.6
		Rostral Anterior Cingulate/Medial Superior Frontal	12.7, 43.8, 14.2

804

805 **Table 5. Significant area differences between groups within Desikan parcels. Area measures in mm^2.**

Parcellation unit	Control	Patient	Significance (p)
Left Cuneus	1900 (+/- 300)	1700 (+/- 280)	0.02
Left Inferior Temporal	4600 (+/- 900)	3900 (+/- 600)	0.01
Left Middle Temporal	4400 (+/- 505)	3900 (+/- 580)	0.01
Left Paracentral	1900 (+/- 400)	1700 (+/- 280)	0.02
Left Postcentral	5400 (+/- 700)	4900 (+/- 670)	0.02
Left Supramarginal	4400 (+/- 810)	4000 (+/- 530)	0.05
Right Inferior Temporal	4500 (+/- 740)	3900 (+/- 560)	<0.01
Right Lateral-occipital	5100 (+/- 750)	4600 (+/- 730)	0.05
Right Precentral	6400 (+/- 800)	5800 (+/- 770)	0.03
Right Superior Frontal	10000 (+/- 1300)	9000 (+/- 1200)	0.02

806

807 **Table 6a: Left hemisphere masked SBM results (p values) between adolescent-onset schizophrenic**
808 **patients and healthy controls.**

Measure	Left Posterior Operculum	Left Inferior Temporal	Left M1	Left SMA
Unscaled				
Mask size	**<0.001**	**0.005**	**0.008**	**0.015**
Surface area	**<0.001**	**0.001**	**0.005**	**0.004**
Metric distortion	**0.015**	0.670	**0.003**	0.870
Mean thickness	0.089	0.360	**0.027**	0.420
Volume	**<0.001**	**<0.001**	**<0.001**	**0.002**
Scaled				
Scaled mask size	**0.001**	**0.007**	**0.015**	**0.027**
Scaled surface area	**<0.001**	**<0.001**	**0.046**	**0.012**
Scaled metric distortion	0.075	0.514	**0.020**	0.510
Scaled thickness	0.150	0.240	**0.042**	0.540
Scaled volume	**<0.001**	**0.001**	**0.001**	**0.004**
Scaled derived volume	**0.007**	0.390	**0.001**	0.980

809

810 **Table 6b: Right hemisphere masked SBM results between adolescent-onset schizophrenic patients**
811 **and healthy controls.**

Measure	Right Posterior Operculum	Right Middle Temporal	Right M1	Right SMA	Right medial frontal/rACC
Unscaled					
Mask size	**0.003**	**0.004**	**0.001**	**0.020**	**0.004**
Surface area	**0.005**	**0.000**	**0.003**	**0.007**	**0.002**
Metric distortion	0.195	0.490	0.110	0.080	0.203
Mean thickness	0.160	0.780	0.120	0.470	0.047
Volume	**<0.001**	**<0.001**	**<0.001**	**0.001**	**0.001**
Scaled					

Scaled mask size	**0.005**	**0.006**	**0.002**	**0.030**	**0.006**
Scaled surface area	**0.047**	**0.000**	0.140	0.060	**0.015**
Scaled metric distortion	0.450	0.170	0.220	0.200	0.093
Scaled thickness	0.230	0.670	0.170	0.580	**0.001**
Scaled volume	**0.001**	**<0.001**	**<0.001**	**0.002**	0.115
Scaled volume change	0.230	0.080	0.123	0.08	**0.030**

*Table 6 Legend: Mask size: voxel count in native space. Volume: approximated mid-thickness area * thickness. Scaled mask size: mask size * average scaling. Scaled thickness: mean thickness * cube root of the average scaling. Scaled area: surface area divided by the mask size^2/3. Scaled volume: the SBM estimated volume * the average scaling. Scaled metric distortion: the mesh triangle area change from the white matter surface to the spherical surface scaled by the ratio of the total surface areas of these surfaces. Scaled volume change: scaled mean thickness divided by the scaled metric distortion. Significant volume differences were corrected for the mask size in the subject's native space.*

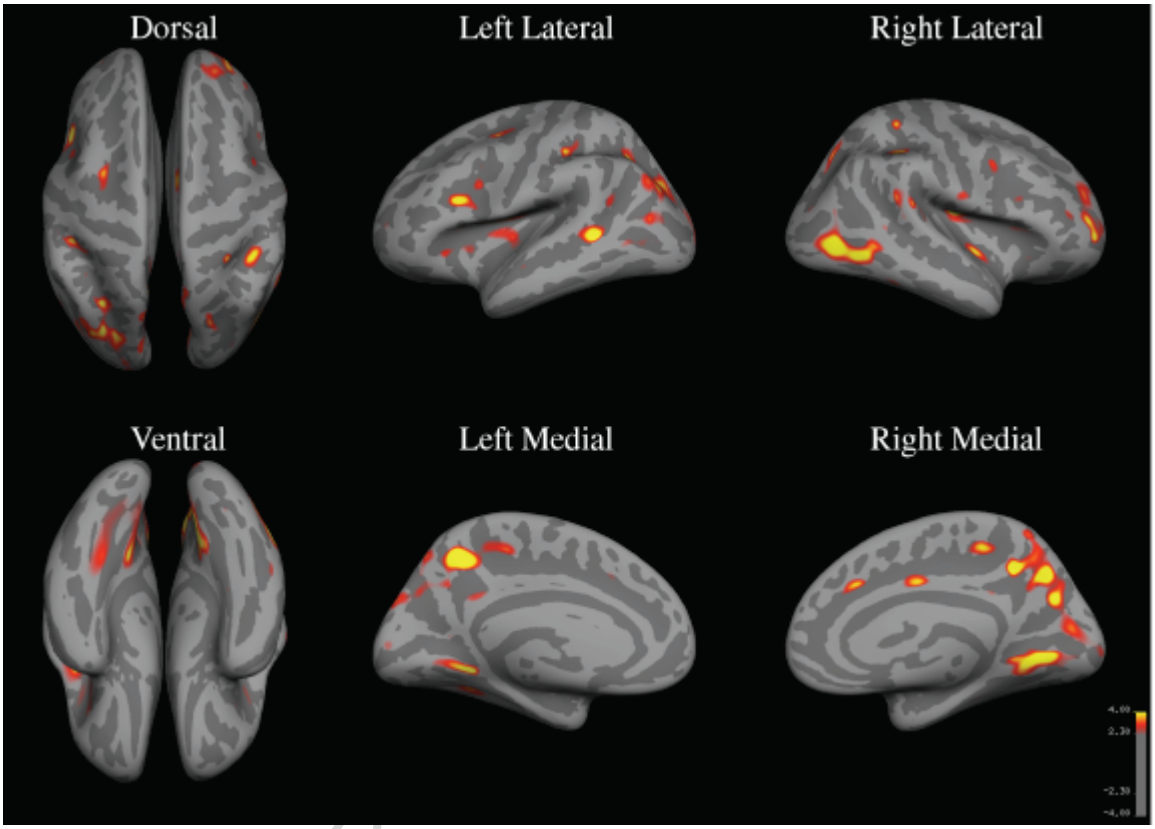

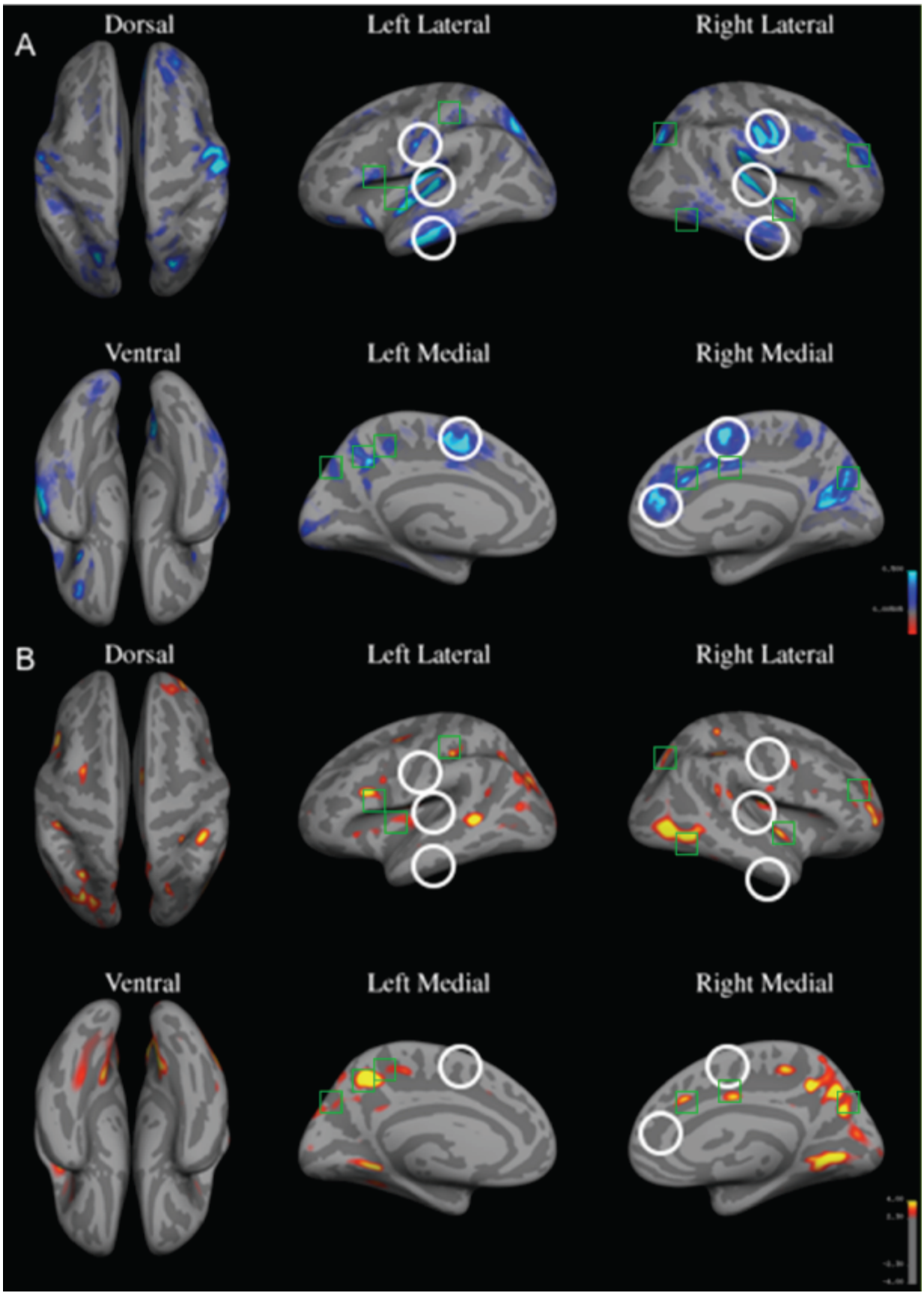
A
Dorsal
Left Lateral
Right Lateral
Ventral
Left Medial
Right Medial
B
Dorsal
Left Lateral
Right Lateral
Ventral
Left Medial
Right Medial